

# Tri-dimensional prostate cell cultures in simulated microgravity and induced changes in lipid second messengers and signal transduction

Sanda Clejan<sup>a\*</sup>, Kim O'Connor<sup>b</sup>, Nitsa Rosensweig<sup>c</sup>

<sup>a</sup> Tulane University School of Medicine, Department of Pathology & Laboratory Medicine and the General Clinical Research Center of Louisiana,

<sup>b</sup> Tulane University, Department of Chemical Engineering,

<sup>c</sup> Xavier University, Department of Chemistry, New Orleans, La., USA

Received: February 15, 2001; Accepted: March 20, 2001

## Abstract

The high aspect rotating-wall vessel (HARV) was designed to cultivate cells in an environment that simulate microgravity. We studied previously the effects of HARV cultivation on DU-145 human prostate carcinoma cells. We determined that HARV cultivation produced a less aggressive, slower growing, less proliferative, more differentiated and less pliant cell than other cell cultivation methods. The result was a 3-dimensional (3D) growth model of prostate cancer which mimics *in vivo* tissue growth. This work examines the signal transduction-second messenger pathways existing temporarily in these HARV cells and correlates these features with the special properties in growth and 3D spheroid formation. We found an initial very active ceramide, a diacylglycerol increase together with increases in PI-PLC and PLA<sub>2</sub> a central defect in PLD (no phosphatic acid or phosphatidylethanol at any time during 15 days of HARV cultivation). There is a cross-talk between ceramide and PI3K pathways with activation of PI3K, after 6 days of HARV growth concomitant with down-regulation of ceramide. At this time, there is also an increase of cAMP (seen by increases in arachidonic acid). Taken together these results can explain the 3D organoid-like growth. We therefore developed a model for growth in HARV prostate cancer cells which involve temporal "switches" between second messengers, activation and cross-talk between multiplicity of signaling pathways and a central defect in PLD pathways. Essential to the late slow growth, and 3D organotypic formation are the apoptotic, anti-survival, anti-proliferation and differentiation pathways in the first days of HARV, with growth of "new" different types of prostate cancer cells which set-up for later "switch" in ceramide-PI3K to survival and proliferation.

## Introduction

Over the past decade a variety of 3-dimensional (3D) prostate cultures were developed as a result of improved methods of cultivation [1]. One of

the most used methods was derived from the advances in microgravity produced by NASA laboratories to cultivate animal cells and especially cancer cells in simulated microgravity for prolonged periods of time. Rotating wall vessels (RWV) developed in these laboratories created a tissue culture system that more faithfully modeled solid tumors as self-assembly into multi-cellular spheroids with highly organized *in vitro* structures with *in vivo* like fidelity [2].

---

\*Correspondence to: Sanda CLEJAN, Ph.D.  
Department of Pathology & Laboratory Medicine,  
Tulane University Health Science Center,  
1430 Tulane Ave., SL 79, New Orleans, LA 70112-2699, USA  
Phone: (504) 586-3865, Fax: (504) 587-7389  
E-mail: sclejan@tulane.edu

Our laboratory previously showed that RWV cultures of DU-145 human prostate carcinoma cells, an androgen independent cell line, were more placid in terms of cell cycle, more differentiated and less pliant than transwell (T. Well) [3]. We then demonstrated that changes in the extent of turbulence and 3D growth contributed to differences in culture performance due to cell-cell and cell-matrix interactions as well as the development of rich interstitial fluid containing growth factors and other biological effectors. We characterized select regulatory and matrix proteins in the high aspect rotating-wall vessel (HARV). For HARV cultures, 3D growth and doubling times were three and 1.5 greater, respectively than for T. Well cultures. By day 17, the ratio of staining intensity for the HARV to that for the T. Well was 0.15 for the epidermal growth factor (EGF), 0.52 for EGF receptor, 1.2 for transforming growth factor (TGF $\beta$ ), 0.52 for EGF receptor, and 0.17 for TGF- $\beta$  receptor, also 3.7 for collagen and 2.4 for laminin. These differences were mediated in part through EGF and TGF- $\beta$ , autocrine loops and cell-cell interactions [4].

Because many of the growth factors and adhesion molecules are linked to intracellular signaling pathways, particular types of growth factors help create the local environmental that determine how a cell will respond to additional signaling molecules and agents [5]. Growth factors changes related to signal transduction help analyze parameters such as differentiation, growth, necrosis, apoptosis, and metastasis [6]. In this paper, we decided to look at some essential initial events in the HARV cells as compared to T. Well, specifically generation of lipid second messengers and the hydrolysis of phospholipids by signaling phospholipases and sphingomyelinases and the activation of membrane associated protein kinases.

## Materials and methods

*Cultivation* - DU-145 (ATCC HTB 81, Rockville, MD) were propagated at 37°C, 95% relative humidity and 5% CO<sub>2</sub> in GTSF-2 medium at pH 7.4 containing 7% fetal bovine serum. Two chambers were used for cultivation: a 50-ml RWV (Synthecon, Houston, TX) called the high aspect rotating-wall vessel (HARV) which was completely filled with medium and has efficient O<sub>2</sub>/CO<sub>2</sub> exchange, and 4.7 cm<sup>2</sup> Transwell-Clear 3450 porous

inserts within a six-well plate (Corning Costar, Cambridge, MA). In the HARV, attachment-dependent DU-145 cells were grown on Cytodex-3 beads (Sigma, St. Louis, MO) at a seeding of five viable cells/bead. The HARV was mixed at 15 rpm. For all chambers, cells were fed to maintain the glucose concentration between 50 and 130 mg/dl, and pH between 7.0 and 7.4 [4].

## Experimental design

In our characterization of HARV cultures of DU-145 cells, the T. Well insert served as control vessel. In T. Well insert, DU-145 cells grew on a flat surface covered with a static layer of medium. This is the typical mode of growth for prostatic cell cultures. As described in our earlier publications HARV cultivation is characterized by end-over-end mixing, bubble-free aeration and solid-body rotation [2]. With these design features, the total hydrodynamic forces acting on a unit area of cell surface in the HARV are estimated to be only 0.2 dyne/cm<sup>2</sup>. For each time of culture (2-14 days), 3 HARV chambers were used, each with the specific radioactive material for the analysis of respectively DAG, ceramide, PA, PE<sub>v</sub>, choline, AA and cAMP. Aliquots were taken for protein or number of cells measurements as described [2]. The chambers were then discarded and new ones were prepared for longer time points. A photograph of HARV can be found in one of our earlier publications [2].

*Determination of diacylglycerol (DAG) levels* - Cellular lipids were extracted as described by Clejan [7]. To eliminate acyl migration of DAG we dried all lipid samples under N<sub>2</sub> in polypropylene vials (poly Q scintillation vials or microfuge tubes; these vials do not release plasticizers when exposed to chloroform/methanol). 1 ml of chloroform was added to the bottom layer, and the solution was then filtered through glass wool in a Pasteur pipette. The collected eluate was evaporated under N<sub>2</sub> at room temperature redissolved in 0.5 ml chloroform, and applied to a 0.5 ml silicic acid column. Neutral lipids were eluted and chromatography was performed as described previously [7]. The standard used was 1,2-DAG (either dipalmitoylglycerol, dioleoylglycerol or 1-stearoyl-2-arachidonoyl-sn-glycerol gave the same standard curve, confirming that this quantitation does not discriminate between lipids based on the number and/or location of double bonds). The detector output was channeled into an analog/digital converter and stored in a computer. Integration of peaks was performed with a CPLIT system.

*Ceramide Analysis* - Ceramide was quantified by the DAG kinase assay as <sup>32</sup>P-incorporated upon phosphorylation of ceramide to ceramide 1-phosphate by DAG kinase as described previously [8]. During initial

examination of measured ceramide levels we used both DAG kinase assay and high pressure liquid chromatographic analysis. These studies were in agreement with the recent publication of Garzotto *et al*, [9] which demonstrated a linear correlation between ceramide generation measured by high pressure liquid chromatography and DAG kinase assay.

*Thin-layer chromatography (TLC) of Phosphatidic Acid (PA)* was previously described [10].

*HPLC of Phospholipids and PA* – Were described previously [11]. Quantitation of PA mass after HPLC was done by a rapid, high sensitive (about 24 OD units/mmol PA) method using complexation with the dye VB. Recovery of added PA was 96%, better than that with TLC methods.

*Transphosphatidylation experiments for demonstration of PLD activation* - To determine activity of PLD, the transphosphatidylation reaction product, phosphatidylethanol ( $PE_t$ ), was measured. PLD catalyzes the transphosphatidylation reaction in the presence of ethanol preferentially to hydrolysis. Cells were pre-labeled with [ $^3H$ ]-myristic acid (1  $\mu$ Ci/ml) for 8 h, and chased in isotope-free medium for 1 h. The lipids from washed cell were extracted by a short-bed/continuous development (SB/CD) TLC using a SB/CD chamber (Regis Chemical Co., Morton Grove, IL) on unmodified silica gel G plates. Cellular PA and  $PE_t$  were resolved using position 5 on the SB/CD chamber for 50 min. and a solvent system of benzene:chloroform:pyridine:formic acid (45:38:4:2.2, v/v) [11].

*Extraction and Analysis of [ $^3H$ ] Choline Labeled Cells* - was described previously [10].

*Radioreceptor assay for inositol trisphosphate ( $IP_3$ )* - was described previously [10].

*Analysis of Phosphoinositides* - HARV and T. Well cells were labeled with [ $^3H$ ] inositol (New England Nuclear, 5-10  $\mu$ Ci/mL, 15 Ci/mM). After 24h of labeling, the cells were placed in a serum-free medium and incubated for an additional 24h. The cells were then harvested in 0.1% HCl in methanol and chloroform was added to separate the phases. The aqueous phase was dried by roto-evaporation and the lipids were deacylated with methylamine reagent (as described previously) [11]. Unbound material was collected and dried by roto-evaporation, resuspended in 10 mM  $(NH_4)_2HPO_4$  (pH 3.8), and analyzed by HPLC as described by Clejan [5], with a Partisphere Sax column (Whatman) and a gradient from 0 to 1.0M  $(NH_4)_2HPO_4$  (pH 3.8) over 120 min. Dual pumps were used to establish the gradient. A second gradient to increase separation of  $IP_3$  was done as described [11]. Eluates from the HPLC column flowed into a continuous flow scintillation detector, and isotope detection data was transmitted to a Power Macintosh 620 for further analysis.

*Analysis of molecular species of DAG, PA, and Phospholipids* - Extracts of DAG were incubated with 3,5-dinitrobenzoyl chloride in dry pyridine at 60°C for 10 min, and the mixture was extracted with *n*-hexane. Butylated hydroxytoluene (10 $\mu$ g) was added to the 2-ml hexane extracts for storage under  $N_2$  prior to HPLC. HPLC was performed as described previously by Clejan [12]. Peaks were identified when possible by reference to published relative retention times [12] using a 16:0, 22:6 FA. Phospholipids (PC, PE, and PI) were separated and purified as described previously [14]. PC, PE, PI were separated into molecular species on a 4.6 X 250 mm Ultrasphere ODS column (Altex Scientific, Inc., Berkley, CA). PC, PE, and PI were eluted with 20 mM choline in methanol:water:acetonitrile (90.5:7:2.5, v/v), at flow rate of 2.0 ml/min. PC and PE were applied to the column in 50-100  $\mu$ l of ethanol and PI in 10-20  $\mu$ l of chloroform. The recoveries of PI, PE and PC were 93.5 to 103%. Likewise, the coefficient of variation of intra- and interassays was below 10% for PE, PC and PI. Within any class of phospholipid, the order of elution of molecular species was constant and entirely dependent on the composition of the component fatty acids. That is, the relative retention time of any particular molecular species was the same in all of the phospholipid classes studied [14].

*Analysis of molecular species of ceramide and sphingomyelin (SM)* was described previously [13].

*$PI_3$ -kinase methods* were performed as described by Susa *et al* [15]. For preparation of total cell extracts 0.5 mL of Nonidet P-40 extraction buffer (25 mM Tris, pH 7.4, 10% glycerol, 1% Nonidet P-40, 50mM NaF, 10 mM sodium pyrophosphate, and protease inhibitors leupeptin and pepstatin at 10  $\mu$ g/mL and apopronin at 5  $\mu$ g/mL) were added to each plate. Cells were left on ice for 5 min., and vortexed for 10 min., spun in a microcentrifuge for 6 min. at 15,000 g, and the total cell extracts from the supernatant aliquoted, frozen in liquid  $N_2$  and stored at -80°C. Cell homogenates were spun in the microcentrifuge for 10 min. The reaction was started by addition of [ $\gamma$ - $^{32}P$ ] adenosine triphosphate (New England Nuclear) at a final concentration of 150 mM (4 mCi/nmol) in a total volume of 50 mL. Incubation was at 37°C for 20 min. Reactions were stopped with 100 mL of 1 M HCl:methanol (1:1, v/v), and phospholipids were extracted twice with the same volume of chloroform.  $^{32}P$ -Labeled phosphatidylinositol (PI) phosphates were resolved by thin-layer chromatography in a solvent system containing water:acetic acid:*n*-propanol (34:1:65, v/v), detected by autoradiography, and  $^{32}P$  incorporation was quantified by liquid scintillation counting as described previously [5].

*Western Blotting for p85* - Protein (60 mg) obtained from HARV and T. Well was resolved by sodium dodecyl sulfate-polyacrylamide gel electrophoresis (SDS-PAGE) (10% acrylamide 0.06% N, N-methylene-bis-acrylamide)

and blotted to polyvinylidene difluoride Millipore membrane using a Bio-Rad Mini Trans-Blot-transfer cell. The membrane was blocked with 5% skimmed milk in TTBS buffer (20 mM Tris, pH 7.4, 100 mM NaCl, and 0.05% Tween-20), and incubated with anti-p85 rabbit antiserum (Upstate Biotechnology, 1:1000 in 1% BSA, TTBS) overnight at room temperature. The blot was washed three times with TTBS and the p85 band was visualized by incubation with  $^{125}\text{I}$ -protein A (New England Nuclear) in 1% BSA, TTBS (130 nCi/mL) for 2h at room temperature and autoradiography. p85 was quantitated by *in situ* densitometry with a Phosphor Imager (Molecular Dynamics) as described previously [5].

**Arachidonic Acid (AA) Release** - Cells were labeled by pre-incubation with 1  $\mu\text{Ci}$  of the  $^{14}\text{C}$  AA per  $0.75 \times 10^5$  cells in GTSF medium for 24 h at  $37^\circ\text{C}$ . Cells were washed three times with 20 ml 0.2% bovine serum albumin to remove free radioactivity. Following this, 2 ml of GTSF was added to HARV and T. Well separate cell cultures and incubated at  $37^\circ\text{C}$ . 50- $\mu\text{l}$  aliquots of incubation media were removed for time-course evaluation of release of  $^{14}\text{C}$  AA, and radioactivity was measured in EcoLite Biodegradable scintillant (ICN, Irvine, CA).

**cAMP measurements** - DU-145 cells from HARV and T. Well were cultured to subconfluence in polylysine-coated six-well culture plates. The attached cells were washed and pre-incubated for 2h in a serum-free basal medium (serum- and bicarbonate-free RPMI-1640 medium containing 10 mM HEPES, pH 7.4; 0.3% BSA; 280  $\mu\text{g}/\text{ml}$  bacitracin; and 10  $\mu\text{g}/\text{ml}$  gentamicin), washed and treated in the presence of 10  $\mu\text{M}$  3-isobutyl-1-methylxanthine for 10 min at  $37^\circ\text{C}$ . Each treatment was performed in triplicate. At the end of the incubation, medium was placed with 1 ml sodium acetate buffer (pH 4.8) and the cells were frozen at  $-80^\circ\text{C}$ , thawed, scraped and transferred to a 1.5 ml tube. The cell lysates were frozen again, thawed, and centrifuged at  $4^\circ\text{C}$  to remove insoluble materials, and the supernatants were stored frozen until the cAMP contents were analyzed by RIA. The cAMP RIA used  $^{125}\text{I}$  2'-O-monosuccinyl-cAMP tyrosylmethyl ester as a tracer, and anti-cAMP rabbit serum was purchased from Biomedical Technologies (Boston, MA). The lower limit of detection for the assay was 0.08 pmol/ml, and the intraassay coefficient of variation among controls was less than 6%. Each was analyzed in duplicate, and all samples from each experiment were analyzed in a single assay to avoid interassay variations.

## Results

We first analyzed the time course of activation of second messenger DAG, which is the endogenous activator of PKC (Fig. 1A) DAG levels peaked in HARV

cultures at 2 days with a 360% increase as compared to control levels. In contrast, DAG increase in T. Well cultures was observed only at day 6 and 8, was more gradual with a maximum of 300% increase compared with control levels. Different curves for activation of the second messenger ceramide were observed (Fig. 1B). In the three experiments, the levels of ceramide varied from one experiment to the other, but the same trend was observed independent of the very different initial levels. Probably subtle changes in feeding (e.g., glucose) and  $\text{O}_2$  account for this phenomenon. T. Well cultures were having near constant levels of ceramide with very gradual increases to day 4, and a similar level (14.8 ng/mg protein) to HARV cultures at day 12 of culture. HARV cultures showed ceramide levels to increase from day 2 to day 6 with a peak 165% higher than T. Well cells, and with a sustained decrease from day 6 to day 12 to the levels in T. Well cultures.

In this study, PA was measured by both TLC and HPLC. PA levels were very low in all HARV timed cultures. In contrast, T. Well cultures showed a maximum PA at day 6, with a gradual decrease but still increased levels above control, even at day 14. In order to determine if PLD was responsible for conversion of phospholipids to PA and DAG, the transphosphatidyl transfer reaction with ethanol and measurements of  $^3\text{H}$   $\text{PE}_t$  were performed (Fig. 2B). As expected from the results with PA, the HARV cultured cells showed no  $\text{PE}_t$ , whereas T. Well cultured cells showed a maximum increase in  $\text{PE}_t$  at 6 and 8 days. The shape of the decreasing curve in  $\text{PE}_t$  (days 10-14) was similar to the PA curve, suggesting  $\text{PE}_t$  is generated at the expense of PA and PLD is active in T. Well cultured cells, but not in HARV cells. In T. Well cultured cells, propranolol treatment enhanced the accumulation of PA and inhibited the formation of DAG (results not shown) in cultures at days 4 to 6, indicating also an active PA-phosphohydrolase in these cells.

HARV cultured cells labeled with  $^3\text{H}$  choline confirmed no activity of PLD by showing no increase in  $^3\text{H}$  choline, only an increase in  $^3\text{H}$  phosphocholine (Table 1). The increase in phosphocholine followed the same temporal pathway as the DAG. In contrast, T. Well cultured cells have first increased  $^3\text{H}$  choline at days 2, 4 and 6 and the increase in phosphocholine at days 8 and 10, showing the presence of both PLD and PLC.

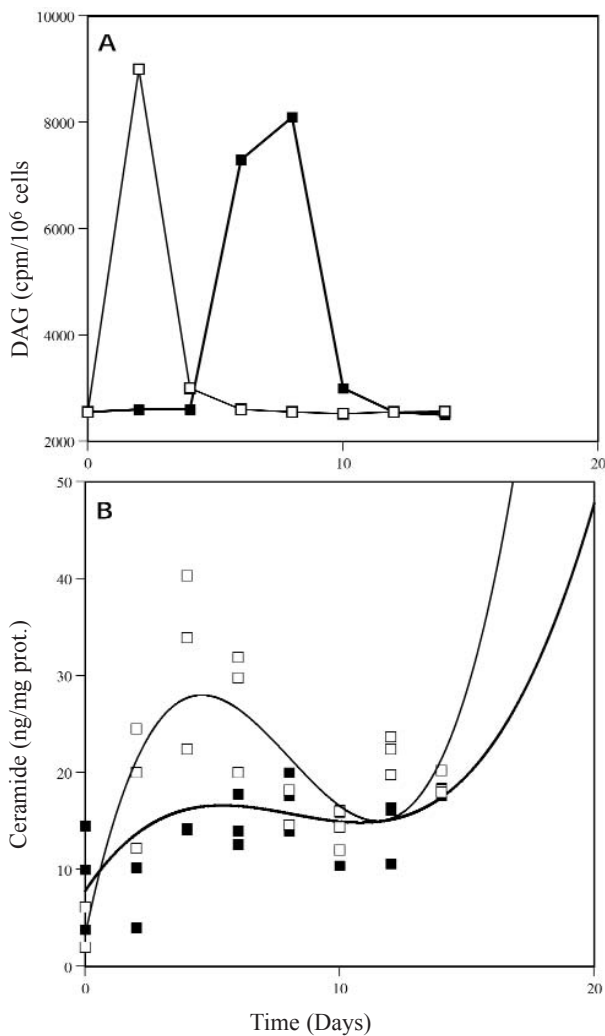


**Fig. 1** Time course of: A) DAG and B) ceramide formation with HARV □—□ and T. Well ■—■ cells. Lipids were extracted at indicated times. Three experiments were performed in triplicate and the mean ± SD was determined for DAG. The best fit data as polynomial third order was determined for ceramide.

In order to understand if early DAG increase in HARV cultured cells was due at least in part to PI-PLC, time dependent production of IP<sub>3</sub> (1,4,5) was measured by radio-receptor assay (Table 2). IP<sub>3</sub> levels in HARV cultured cells rose rapidly at 2 days and fell as rapidly to non-measurable levels. In contrast, T. Well cultured cells rose slightly at days 2 to 4, and gradually increased to day 10.

Typical elution profile of radio-labeled inositol metabolites from anion exchange HPLC (Table 3) showed effects for HARV cultured cells at the 2

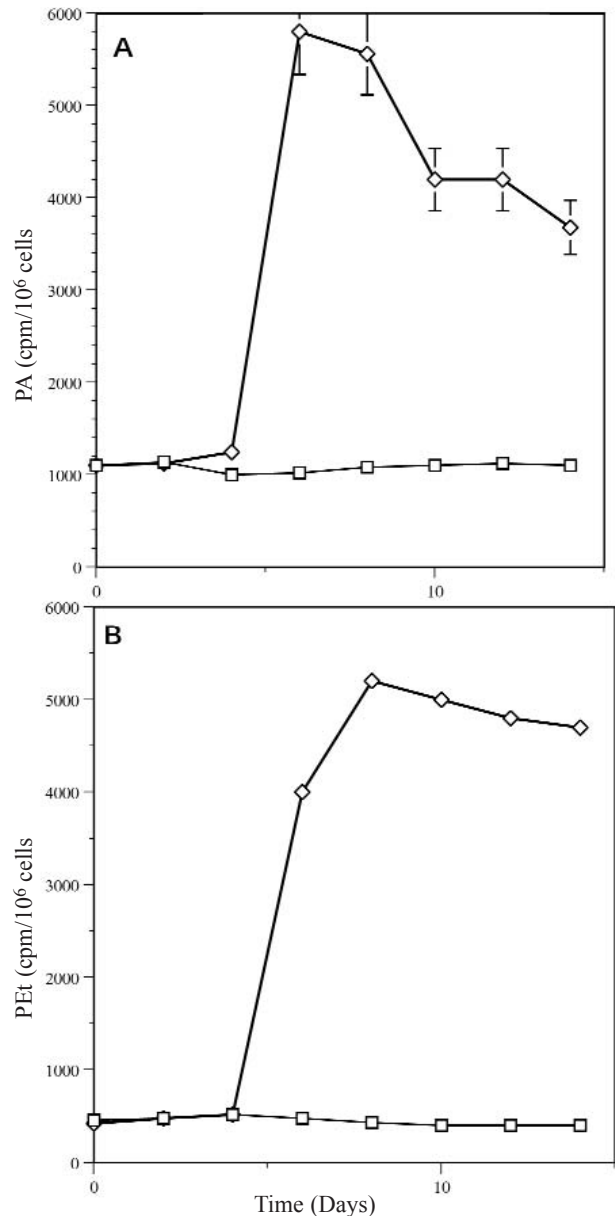


**Fig. 2** Changes in lipid second messenger PA (A) and formation of [<sup>3</sup>H] PET in the presence of ethanol (B) with HARV □—□ and T. Well ◇—◇ cells. Cells were pre-labeled with [<sup>3</sup>H] myristic acid as described in section 2 in the presence and absence of ethanol. Lipids were extracted and [<sup>3</sup>H] PA and [<sup>3</sup>H] PET determined. Three separate experiments in triplicate and the mean ± SD was determined.

days also, with increased IP<sub>3</sub> (1,4,5) levels and PIP<sub>2</sub> decrease, consistent with PI-PLC activity. The most dramatic changes were apparent in PIP<sub>3</sub> (3,4,5) which were not detected at all at time 0-4 days of culture, but increased slowly thereafter to day 12.

**Table 1** Temporal effect of culture conditions on IP<sub>3</sub> accumulation in HARV and T. Well grown cells.

Culture Time (days)	PI <sub>3</sub> Levels (pmols/10 <sup>6</sup> cells)	
	HARV	T. Well
0	18.4 ± 2.6	14.6 ± 3.2
2	52.2 ± 4.3	17.4 ± 1.9
4	18.0 ± 3.0	20.2 ± 2.6
6	10.4 ± 2.2	24.8 ± 3.0
8	--	29.9 ± 2.4
10	--	33.5 ± 4.2
12	--	32.0 ± 3.4
14	--	29.8 ± 4.0

A very small trace of PIP<sub>3</sub> (3,4,5) was seen constantly in cultured T. Well cells (results not shown). These elution profiles suggested a low PI<sub>3</sub> kinase activity in T. Well cultures and an increase in such activity in HARV cultured cells only at 10 days of culture. Since the analysis of levels of phosphoinositides in cells require large amounts of radio labels, and since the HPLC quantitation of the lipids was variable between separate experiments, we used a PI<sub>3</sub> kinase assay which measured functional kinase activity directly on cell extracts.

Directly assayed PI<sub>3</sub> kinase activity (Fig. 3B) showed exactly the same behavior as p85 protein

measured by immunoassay Western blot (Fig. 3A): mostly constant levels in T. Well cultured cells independent of time of culture in both PI<sub>3</sub> kinase and p85 protein, and low p85 to very low PI<sub>3</sub> kinase levels in the first days of culture (0-6 days) with a burst of increase late (10-12 days). Thus, the decrease or increase in p85 maybe precisely correlated with PI<sub>3</sub> kinase activity.

In an attempt to better understand the temporal increase in DAG in HARV and T. Well cultured cells, and increases in PA in T. Well cultured cells and the nature of the hydrolysis of phospholipids by phospholipases, an analysis of molecular species of

**Table 2** [<sup>3</sup>H] Choline and [<sup>3</sup>H] Phosphocholine release by HARV and T. Well grown cells.

Culture Time (days)	[ <sup>3</sup> H] Choline cpm/10 <sup>6</sup> cells		[ <sup>3</sup> H] Phosphocholine cpm/10 <sup>6</sup> cells	
	H	TW	H	TW
0	1110 ± 78	1096 ± 112	684 ± 92	592 ± 11
2	1096 ± 82	6820 ± 128	9384 ± 68	638 ± 122
4	1140 ± 112	7372 ± 105	1070 ± 112	700 ± 139
6	1044 ± 98	8020 ± 164	680 ± 102	626 ± 104
8	1034 ± 148	1130 ± 98	708 ± 86	5426 ± 8
10	1200 ± 140	1162 ± 82	690 ± 90	6104 ± 10
12	1124 ± 126	1204 ± 108	684 ± 88	1830 ± 12
14	1096 ± 88	1188 ± 78	650 ± 114	696 ± 13

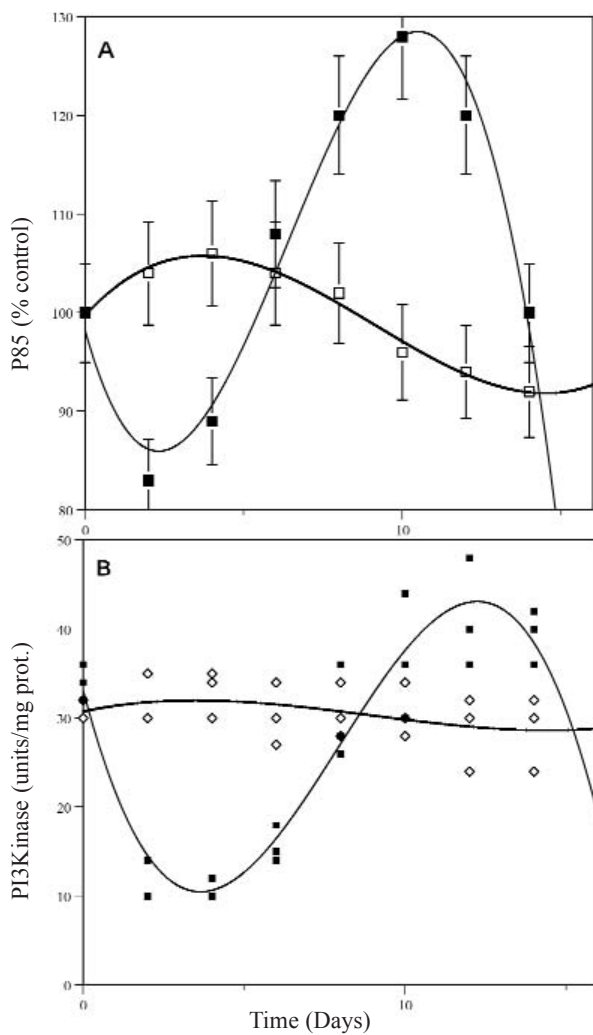


**Fig. 3** Effects of growth conditions on p85 protein (A) and PI3K activity (B). HARV cells  $\square$ — $\square$  and T. Well cells  $\blacksquare$ — $\blacksquare$ .

PC, PE, PI and DAG (Table 4) or PA and phospholipids (Table 5) were made by HPLC and TLC. We identified only 7 species of DAG and PA, which increased non-uniformly from a total of 18 molecular species existent in DU-145 cells. We found decreases of more than 1% in molecular species of phospholipids, mostly PI and PC, and to smaller extent, PE. The DAG molecular species 16:0, 20:4; 16:0, 18:2; 18:1, 18:2; 18:0, 22:6 and 18:0, 20:4 which were increased in HARV cultured cells, corresponded mostly to decreases in PI. Only the 16:0, 18:2 pair showed a more pronounced increase in PC. The source of fatty acid at the time of maximum increase in DAG in T. Well cultured cells

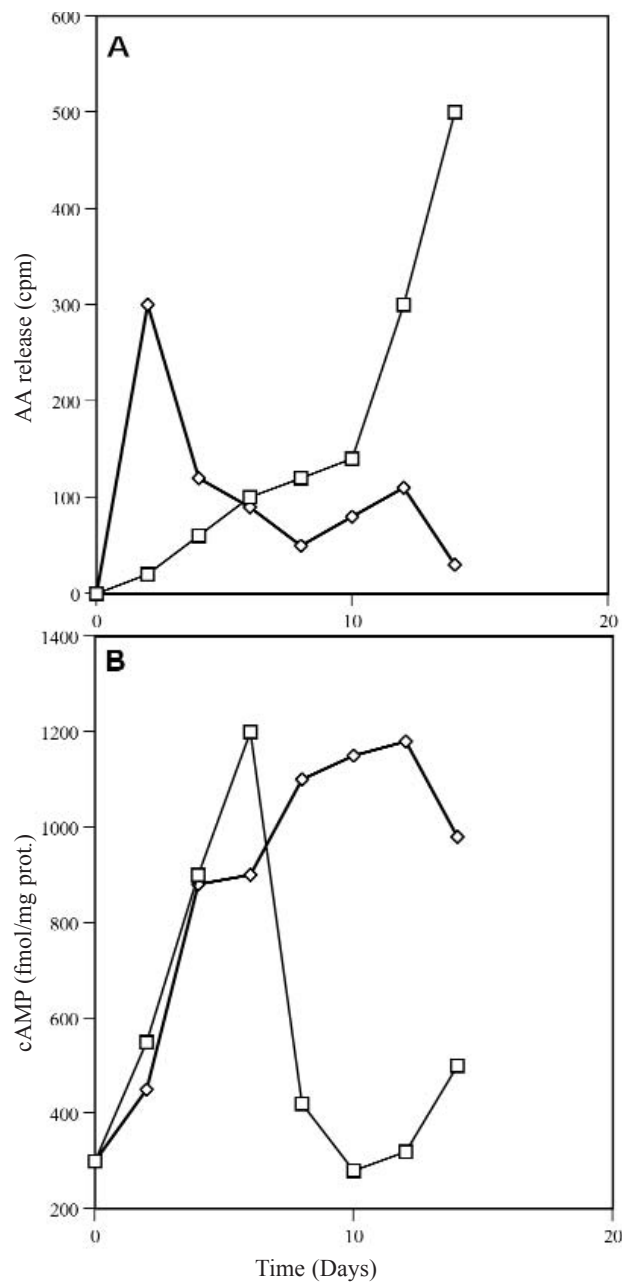


**Fig. 4** Time dependent release of  $[^{14}\text{C}]$  AA (A) and cAMP (B). HARV  $\square$ — $\square$  and T. Well  $\diamond$ — $\diamond$ .

changed markedly with more increase in PC molecular species than PI molecular species, and no change in PE (Table 4). The increase in PA molecular species (Table 5), which was observed only in T. Well cultured cells and not in HARV, showed fewer changes in the number of molecular species (only 3) and these changes correspond to more pronounced decreases in PI than PC.

**Table 3** Typical elution profile from anion-exchange HPLC analysis of deacylated and deglycerated [<sup>3</sup>H] Inositol-labeled lipids of HARV cultured cells.

Culture Time (days)	IP <sub>2</sub>	PIP <sub>2</sub>	IP <sub>3</sub> (1,3,4) cpm	IP <sub>3</sub> (1,4,5)	PIP <sub>3</sub> (3,4,5)
0	506	1860	1200	984	639
2	492	960	1508	4128	474
4	510	986	1636	1062	396
6	484	890	1222	966	636
8	463	928	1193	960	2480
10	477	938	1162	976	3726
12	492	910	1175	943	4543
14	500	922	1100	950	2430

As the total ceramide temporal release was very different in HARV grown cells compared with T. Well grown cells, and as there are different agents to induce hydrolysis of sphingomyelin (SM) by a sphingomyelinase (SMase) with the final effect of induction of cell differentiation and/or apoptotic death, an accurate and simultaneous determination of molecular species of both SM and ceramide was important. Table 4 shows the major FA composition first and the long chain base composition second. Only three different molecular species were showing major changes with an increase in ceramide and proportional decreases in SM with temporal change

at 2 and 6 days of HARV culture. The first chain in these changed FA is saturated (16:0 or 18:0) and unusually one monounsaturated long chain (24:1). The only sphingoid base presented in all 3 molecular species is C 18-sphinganine (18:1) base.

Activation of PLA<sub>2</sub> and AA release and metabolism are important mechanisms of signaling in prostatic adenocarcinomas. DU-145 prostate epithelial cells from HARV cultures (Fig. 4A) showed a gradual increase in the rate of release of [<sup>14</sup>C] AA at 2-10 days of culture and a subsequent sustained higher release over the 10-14 days of culture. In contrast, the T. Well grown cells had a biphasic increase

**Table 4** Changes in the molecular species of DAG and phospholipids in HARV and T. Well cultured cells, at the maximum increase in total DAG (2 and 10 days respectively).

Molecular Species	Mole % Change							
	HARV/2 days				T. Well/10 days			
	DAG	PC	PI	PE	DAG	PC	PI	PE
16:0, 20:4	+2.2	-1.0	-1.8		+3.1	-2.4	--	-1.0
16:0, 18:2	+2.4	-3.6	-3.0		+1.0	-1.6	--	--
18:1, 18:2	+2.4	--	-3.8		--	--	--	--
18:0, 22:6	+2.2	--	1.8		+2.6	--	-2.0	--
18:0, 20:4	+3.4	-1.5	-4.6	-1.2	+3.0	-2.6	--	-0.8
18:0, 18:1	--	--	--	--	+1.6	-1.3	--	--



**Table 5** Changes in the molecular species of PA and phospholipids in T. Wells cultured cells at maximum increase in total PA

Molecular Species	Mole % Change		
	PA	PI	PC
18:0, 20:4	+3.0	-2.5	-1.1
18:0, 18:1	+2.8	-3.0	--
18:1, 20:4	+4.2	-2.6	-1.8

in the rate of release peaking at 2 days, followed by re-uptake of radioactivity at 4-6 days and a smaller peak at 12 days. As the DU-145 prostate carcinoma cells express, focal neuroendocrine differentiation which is partially mediated through cAMP activation of signaling mechanisms, we measured cAMP in both HARV and T. Well grown cultures. Fig. 4B shows a continuous increase in the cAMP generated by HARV grown cells with the maximum at day 12, whereas T. Well grown cells showed a 90% increase of cAMP at day 6, and a sharp decrease thereafter.

## Discussion

We have developed two cell models of prostate cancer with which to compare and investigate the molecular basis of highly organized 3D-structure, self-aggregation, cell proliferation and differentiated function [2]. Both models are cultures of DU-145 human prostate carcinoma cells: one is grown as tissue-like spheroids; the other, as a cellular bilayer. The spheroids behave as well-differentiated

solid tumors, while the bilayer behaves as an aggressive invading tumor margin. The spheroids are more differentiated, are slower growing, have greater cytoskeletal and extracellular organization, and have far different staining intensities for autocrine growth factors and their receptors [4].

In this study, we are using the spheroid/bilayer system to investigate during physiological stimulation, the signal transduction associated with the lipid second messengers AA, DAG, PA, ceramide and phospholipase A<sub>2</sub> (PLA<sub>2</sub>), phospholipase C (PLC), phospholipase D(PLD), PI<sub>3</sub> kinase (PI<sub>3</sub>K), SMase and cAMP. Our aim was to determine the early signal transduction pathways without supplementation of the culture medium with additional hormones or growth factors. This was based on our previous studies which implied at least EGF and TGF- $\beta$  autocrine growth factor regulation mediated HARV-induce changes [4]. The expression of TGF receptor and ligand in both HARV and T. Well, the increased activity of TGF in HARV and EGF in T. Well culture, made us try to map the early signal transduction pathways without additional supplementation of what the fetal calf serum contained.

**Table 6** Changes in the molecular species of ceramide and sphingomyelin in HARV at 2 and 6 days of culture.

Molecular Species	Mole % Change			
	2 days		6 days	
	SM	CER	SM	CER
16:0, 18:1	-1.6	+0.6	-2.5	+5.2
18:0, 18:1	-3.8	+4.0	-3.0	+5.4
24:1, 18:1	-2.6	+3.3	-4.0	+2.8

We also correlated the different signal transduction pathways with the temporal increase or decrease in growth, proliferation, invasiveness, differentiation (morphologic and neuroendocrine), apoptosis and necrosis.

We found a multiplicity of pathways involved, a highly redundant system of cell regulation, characteristic cross-talk between different second messengers which shedded light on the 3D-structure of spheroids.

The increase in DAG, which occurs within the first 2 days of HARV culture (Fig. 1A), was coincident within an increase in  $IP_3$  production (Table 1). Examination of HARV individual molecular species of DAG and phospholipids revealed a selective increase in PI-derived DAG (Table 4) and very little increase in PC-derived DAG. The reverse is true for T. Well cultured cells at maximum increase in DAG (8 and 10 days), where most DAG was derived from PC than PI molecular species. Thus, PI is a major source of DAG in HARV, and  $PI_3$  increase showed an active PI-PLC in HARV culture immediately after initiation of HARV culture. Some but more limited PLC hydrolysis is produced from PC as shown by the decrease in PC molecular species and also in an increase of phosphocholine at 2 days of culture (Table 2). In T. Well cultures, most of the increase in DAG (days 8 and 10) is due to hydrolysis of PC by PLC, although some PI-PLC activity is available to the cells, shown by some small increase in  $IP_3$  and decrease in 1 molecular species of PC [Table 4]. Therefore, the preferential pathway involves PI-PLC in HARV, but PC-PLC in T. Well culture. Examination of the temporal effects of culture conditions on both PA levels and  $PE_t$  after transphosphatidylation [Figs. 2A and B] showed, at no time during culture, any increase in HARV, either in PA or  $PE_t$ . Thus, no activation of PLD was seen. The production of  $PE_t$  in T. Wells cultured cells corresponding to increase in PA at 6 and 8 days suggest an activation of PLD, albeit later in these cells. Thus, in HARV cultured cells, a defect in central signal transduction pathways were traced to a defect in an upstream target-PLD. Also, in T. Well cultured cells DAG produced at day 10 was due to a PLD - PA phosphohydrolase pathway as confirmed by the measurement of PA and DAG in the presence of propanolol an inhibitor of PA phosphohydrolase. Therefore, in T. Well cells most PA

may be generated through PLDs through an active PA-phosphohydrolase and active PLD. In T. Well cells, PLD is demonstrated also by the increase in choline, especially at day 6 of culture. Also through an increase in phospholine (day 10) and the changes in molecular species of PC, a PC-PLC is active albeit later than in T. Well cell cultures. Moreover,  $IP_3$  [Table 3] increase in T. Well cells demonstrates also an active PI-PLC, at least later (days 8-10). So, the picture in T. Well grown cells shows: 1) a multiplicity of pathways; 2) increased cross-talk between DAG and PA, PI-PLC and PC-PLC and PC-PLD. The mechanism of inhibition of some of these pathways, especially PLD in HARV cells may be due to the presence of a dominant inhibitor of PLD and/or HARV grown cells may be missing the ADP ribosilation factor [8]. More probable our results confirm the presence of such an inhibitor in HARV [11]. Indeed the activation of ceramide is very different in HARV than in T. Well [Fig. 1B]. The increase in ceramide compared to T. Well is seen at initiation of the culture and continues with a peak to 6 days. Only on day 12, does HARV have the same low ceramide level as T. Well grown cells, but then the ceramide increased again in HARV. Thus, in HARV ceramide produced a growth arrest effect and mediated apoptosis early, and then later induced differentiation. The cross-talk between ceramide pathway and DAG cycle increased the complexity of signaling pathways leading to late proliferation and additional sites of regulation. Changes in the molecular species of ceramide in HARV at different ages of culture are in themselves interesting with a preponderance of monounsaturated 18:1 species (sphinganine) present in the sphingoid base, and only three FA long chain (16:0, 18:0 and 24:1) present. The most peculiar feature is the relative high proposition of 24:1, 18:1 pair, which increase in ceramide and decrease in sphingomyelin in DU-145 HARV-grown cells and increase with age of the culture also in DMSO treated neuroblastoma NIE-115 cells [16]. Also, in this cell model 18:0, 18:1 ceramide molecular species increased with morphological differentiation.

$PI_3K$  has emerged as a critical signaling molecule that regulates multiple cellular processes including survival and proliferation in numerous systems.  $PI_3K$  is composed of regulatory p85 subunit and a catalytic p110 subunit that as an active

complex phosphorylate the 3-ring position of PI-4,5-bisphosphate to generate PI-3,4,5-triphosphate (PIP<sub>3</sub>) [17]. Downstream targets activated subsequent to PIP<sub>3</sub> include PKC isoforms, JNK, Ras, p70 S6 kinase, Rac, and PKB/Akt of which PKB/Akt has been implicated as an intermediate in PI<sub>3</sub>K generated survival signals. Known activators of PI<sub>3</sub>K, including the peptide hormones PDGF, NGF, and IGF-1 as well as PMA act as survival factors suppressing apoptosis induced by a number of agents [18-21]. Additionally, transfection of cells with constitutively active PI<sub>3</sub>K or Akt results in inhibition of apoptosis induced by c-Myc, UV radiation, TGF-β as well as Fas [15-21]. PI<sub>3</sub>K activation of Akt/PKB and subsequent phosphorylation of Bad suggests one mechanism by which PI<sub>3</sub>K signaling acts to suppress apoptosis [22-24]. However, others [25] have demonstrated PKB/Akt survival signaling can occur independently of Bad phosphorylation, suggesting that the PI<sub>3</sub>K survival signal may target multiple components of the apoptotic cascade. Recently, ceramide has been shown to suppress Akt/PKB and its survival signaling suggesting cross-talk between these two pathways [17, 26-28]. Based upon this information, we examined both the ability of a PI<sub>3</sub>K signal to suppress apoptosis as well as the coordinate cross-regulation between the PI3K and ceramide pathways in HARV. Such cross-talk between PI<sub>3</sub>K and sphingomyelinase pathways as a mechanism for cell survival/death decision was demonstrated by us in a breast cancer cell line MCF-7 [6]. We detected first in HARV grown cells, a decrease in PIP<sub>3</sub> [2-4 days] with a gradual increase (days 6-10) [Table 3]. This was confirmed by both measurements of PI<sub>3</sub>K and p85 (Fig. 3A and B). This behavior of PI<sub>3</sub>K thus activates survival signaling intermediates in HARV at a very specific time of growth. The importance of ceramide as an early intermediate for cell death signaling and the suppression of ceramide generation by PI<sub>3</sub>K regulation was previously demonstrated in other cell types [5, 6, 16, 29]. We suggest that molecular suppression of the PI<sub>3</sub>K cascade occurs in HARV grown-cells in early phases (2, 4, 6 days) either through direct regulation of the duration of SMase activation or at levels

occurring subsequent to the generation of ceramide. PGF-induced ceramide levels is suggestive of additional signaling pathway in addition to PI<sub>3</sub> kinase-like PI-PLC, but no PLD. Thus, these results suggest that the regulation of ceramide levels within HARV-cells may be dependent both on activation of cell stress and apoptotic inducers, as well as through survival factors activating negative regulatory pathways that keep ceramide levels in check. We propose that ceramide acting as a cellular stress response intermediate alone, is insufficient to induce apoptosis in HARV.

This is consistent with the suggestion that PGF-induced apoptosis occurs primarily through a TNFR1-TRADD-Fas-associated death domain-caspase activation [6]. However with the suppression of PI<sub>3</sub>K, the prolonged and enhanced ceramide signal is capable of functioning to promote apoptosis. In contrast, overactivation of the PI<sub>3</sub>K pathway suppressed the ceramide signal thereby facilitating cell survival. It is therefore interesting to speculate that it is the relative balance between these two early lipid signaling pathways that in part determines the outcome of cell survival/death decisions and ultimately 3D growth in HARV.

Given the convincing role of ceramide in numerous cellular processes as a stress signal mediator and the role of PI<sub>3</sub>K in cell survival and proliferation decisions we propose a more universal role for these two signals as a part of the cellular machinery which regulates early lipid signaling events, the output of which determines the fate of the cell, and in HARV cells, the fate and extent of 3D growth.

The study of AA and cAMP in HARV-compared with T. Well-grown cells (Fig. 4A, B) add an additional level of cross-talk probably responsible for the fine-tuning of 3D growth. Eicosanoids, a plethora of chemically different metabolites arising from the oxidation of AA, constitute an important family of regulators of signal transduction in HARV. A role for activation of PLA<sub>2</sub> and AA release in tumor growth invasiveness, and metastasis have been suggested [30] as well as a role for AA metabolites in endothelial cell and smooth muscle cell regulation of vascular growth. It is tempting to speculate that the characteristic pattern of AA stimulation in HARV cells late in the process, after earlier apoptosis and reverse differentiation and increase 3D growth later corresponding to the highest increase

in AA, stimulates prostate tumor invasiveness, albeit late in the process. Accumulating evidence suggest that cAMP in prostate cancer regulates the neuroendocrine differentiation [31], induce G<sub>1</sub> synchronization, growth arrest and loss of clonogenicity, indicating terminal differentiation [32]. Our data of the temporal relation in HARV with increase in cAMP to 6 maximum 8 days, thus will indicate at this time plasticity in the lineage commitment and neuronal morphology.

## Conclusions

The signal transduction model found herein begins to describe the dynamics of 3D growth in HARV under microgravity condition for DU-145 prostate cancer cultures. The features most important: a) initial slow growth, b) 3D organization, c) differentiated function of like intact tissue are all determined by the temporal events initiated immediately after the first hours of HARV cultures. Due to increased cell-cell and cell-matrix interactions as well as the development of a rich interstitial fluid containing growth factors (especially TGF and EGF) in the first two days, a “switch” between signal transduction pathways is happening. First, our results indicate inactivation of PLD while activating PI-PLC, PLA<sub>2</sub> and SMase pathways. The ceramide increase and the ceramide/DAG signals point out to apoptosis in these cancer cells, increase differentiation signals or what can be defined as reverse transformation in the first 6 days of growth. Due to PLA<sub>2</sub> activation, and thus activation of prostaglandins and eicosanoids (pro-inflammatory mediators), “new” DU-145 cancer cells with different features are growing. The cross-talk between PI<sub>3</sub>K and SMase pathways is also very important for initial decrease survival and proliferation (with low PI3K to day 6) and PI<sub>3</sub>K activation after day 6 and thus increase proliferation and survival of “new” DU-145 cells with differentiated function. Even after day 6, the complete central defect in PLD implied that some pathways of growth are not available for HARV cells. These “new” DU-145 cells will have an increase in cAMP which restore integrity of a few regulatory pathways and select specific regulatory and matrix proteins to grow. Then, we find down-regulation and then up-regulation of the expression

or function of adhesion molecules for 3D growth and formation of an extensive, complex basement membrane extracellular matrix. Therefore, it appears a 3D organotypic structure in HARV cultures under microgravity conditions arises only after: 1) temporal “switches” between second messengers and 2) extensive cross-talk between a multiplicity of activated signaling pathways .

This model of signal transduction found for HARV DU-145 prostate cancer of how are the molecular signals integrated among growth factors, extracellular matrices and intracellular receptors has to be examined in other spheroid/grown cancer and non-cancer systems, to confirm a more generalized model of signal transduction in different spheroid cultures.

## Acknowledgements

This research was supported by grants from NIH-GCRC #5M01 RR5096-10 (SC), Department of Defense (DOD) (SC) and NASA (KO). We are grateful to Mr. Robert Mazzola and Dr. Robert Dotson for technical assistance, and Corlis M. Trepagnier for her assistance in the preparation of this manuscript.

## References

1. **O'Connor K.C.**, Three-dimensional cultures of prostatic cells: tissue models for the development of novel anti-cancer therapies, *Pharm. Res.*, **16**: 486-493, 1999
2. **Clejan S., O'Connor K.C., Cowger N.L., Cheles M.K., Haque S., Primavera A.C.**, Effects of simulated microgravity on DU-145 human prostate carcinoma cells, *Biotech. Bioeng.*, **50**: 587-597, 1996
3. **O'Connor K.C., Enmon R., Primavera A., Dotson R. Clejan S.**, Characterization of extracellular matrix in three-dimensional cultures of DU-145 human prostate carcinoma cells. In: MJT Carrondo, JB Griffiths, C MacDonald, eds., *Animal Cell Technology, Vaccines to Genetic Medicine*, Kluwer Academic Publishers, Dordrecht, 1996, pp. 571-575
4. **O'Connor K.C., Enmon R.M., Dotson R.S., Primavera A.C., Clejan S.**, Characterization of autocrine growth factors, their receptors and extracellular matrix present in three-dimensional cultures of DU-145 human prostate carcinoma cells grown in simulated microgravity, *Tissue Eng.*, **3**: 2,161-171, 1997

5. **Clejan S., Dotson R.S., Ide C.F., Beckman B.S.**, Coordinated effects of electromagnetic field exposure on erythropoietin-induced activities of phosphatidylinositol-phospholipase C and phosphatidylinositol 3-kinase, *Cell. Biochem. Biophys.*, **27**: 203-225, 1997
6. **Burrow M.E., Weldon C.B., Collins-Burrow B.M., Ramsey N., McKee A., Klippel A., McLachlan J.A., Clejan S., Beckman B.S.**, Cross-talk between phosphatidylinositol 3-kinase and sphingomyelinase pathways as a mechanism for cell survival/death decisions., *J. Biol. Chem.*, **275**: 13;9628-9635, 2000
7. **Clejan S.**, Analytical methods and steps to sample preparation for determination of molecular species of fatty acids. In: Bird I.M. and Clejan S, eds., *Molecular Biology, Phospholipid Signaling Protocols*, Humana Press, vol. 105, New Jersey, 1998, pp. 243-254
8. **Burow M.E., Weldon C.B., Tang Y., Navar G.L., Krajewski S., Reed J.C., Hammond T.G., Clejan S., Beckman B.S.**, Differences in susceptibility to tumor necrosis factor  $\alpha$ -induced apoptosis among MCF-7 breast cancer cell variants, *Cancer Res.*, **58**: 1, 4940-4946, 1998
9. **Garzotto M., White-Jones M., Jiang Y., Ehleiter D., Liao W.C., Haimovitz-Friedman A., Fuks Z., and Kolesnick R.**, 12-O-tetradecanoylphorbol-13-acetate-induced apoptosis in LNCaP cells is mediated through ceramide synthase, *Cancer Res.*, **58**: 2260-2264, 1998
10. **Clejan S., Ide C., Walker C., Wolf E., Corb M., and Beckman B.**, Electromagnetic field induced changes in lipid second messengers, *J. Lipid Med. Cell. Sig.*, **13**: 301-324, 1996
11. **Clejan S., Mallia C., Vinson D., Dotson, R, and Beckman B.S.**, Erythropoietin stimulates G-protein-coupled phospholipase D in haematopoietic target cells, *Biochem. J.*, **314**: 853-860, 1996
12. **Clejan S.**, HPLC analytical methods for the separation of molecular species of fatty acids in diacylglycerol and cellular phospholipids. In: Bird I.M. and Clejan S, eds, *Methods in Molecular Biology, Phospholipid Signaling Protocols*, Vol. 105, Humana Press, New Jersey, 1998, pp. 255-274
13. **Clejan S.**, Analysis of molecular species of cellular sphingomyelins and ceramides. In: Bird I.M. and Clejan S, eds, *Methods in Molecular Biology, Phospholipid Signaling Protocols*, Vol. 105, Humana Press, New Jersey, 1998, pp. 275-285
14. **Beckman B.S., Mallia C., Clejan S.**, Molecular species of phospholipids in a murine stem cell line responsive to erythropoietin, *Biochem. J.*, **314**: 861-867, 1996
15. **Susa M., Keeler M., Varticovski L.**, Platelet-derived growth factor activates membrane-associated phosphatidylinositol 3-kinase and mediates its translocation from the cytosol, *J. Biol. Chem.*, **267**: 22, 951-956, 1992
16. **Clejan S., Wolf E., Corb M., Dotson R., Ide C.**, Morphological differentiation of N1E-115 neuroblastoma cells by dimethyl sulfoxide and activation of lipid second messengers, *Exp. Cell. Res.*, **224**: 16-27, 1996
17. **Coffer P.J., Jin J., Woodgett J.R.**, Protein kinase B (c-Akt): a multifunctional mediator of phosphatidylinositol 3-kinase activation, *Biochem. J.*, **335**: 1-13, 1998
18. **Downward J.**, Mechanisms and consequences of activation of protein kinase B/Akt, *Curr. Opin. Cell. Biol.*, **10**: 262-267, 1998
19. **Kulik G., Weber M.J.**, Akt-dependent and -independent survival signaling pathways utilized by insulin-like growth factor 1, *Mol. Cell. Biol.*, **18**: 6711-6718, 1998
20. **Dudek H., Datta S.R., Franke T.F., Birnbaum M.J., Yao R., Cooper G.M., Segal R.A., Kaplan D.R., Greenberg M.E.**, Regulation of neuronal survival by the serine-threonine protein kinase Akt, *Science*, **275**: 661-665, 1997
21. **Chen R.-H., Su Y.-H., Chuang R.L.C., Chang T.-Y.**, Suppression of transforming growth factor-beta-induced apoptosis through a phosphatidylinositol 3-kinase/Akt-dependent pathway, *Oncogene*, **17**: 15,1959-1968, 1998
22. **Eves E.M., Xiong W., Bellacosa A., Kennedy S.G., Tsichlis P.N., Rosner M.R., Hay N.**, Akt, a target of phosphatidylinositol 3-kinase, inhibits apoptosis in a differentiating neuronal cell line, *Mol. Cell. Biol.*, **18**: 4,2143-3252, 1998
23. **Cuvillier O., Rosenthal D. S., Smulson M. E., Spiegel S.**, Sphingosine 1-phosphate inhibits activation of caspases that cleave poly (ADP-ribose) polymerase and lamins during Fas- and ceramide-mediated apoptosis in Jurkat T lymphocytes, *J. Biol. Chem.*, **273**: 5,2910-2916, 1998
24. **Datta S.R., Dudek H., Tao X., Masters S., Fu H., Gotoh Y., Greenberg M.E.**, Akt phosphorylation of BAD couples survival signals to the cell-intrinsic death machinery, *Cell*, **91**: 2,231-241, 1997
25. **Scheid M.P., and Duronio V.**, Dissociation of cytokine-induced phosphorylation of Bad and activation of PKB/akt: involvement of MEK upstream of Bad phosphorylation, *Proc. Natl. Acad. Sci. USA*, **95**: 13,7439-7444, 1998
26. **Zundel W., Giaccia A.**, Inhibition of the anti-apoptotic PI(3)K/Akt/Bad pathway by stress, *Genes Dev*, **12**: 13,1941-1946, 1998
27. **Summers S.A., Garza L.A., Zhou H., Birnbaum M.J.**, Regulation of insulin-stimulated glucose transporter GLUT4 translocation and Akt kinase activity by ceramide, *Mol. Cell. Biol.*, **18**: 9,5457-5464, 1998
28. **Zhou H., Summers S.A., Birnbaum M.J., Pittman R.N.**, Inhibition of Akt kinase by cell-permeable ceramide and its implications for ceramide-induced apoptosis, *J. Biol. Chem.*, **273**: 26,16568-16575, 1998

29. **Dufourny B., Alblas J., van Teeffelen H.A., van Schaik F.M., van der Burg B., Steenbergh P.H., Sussenbach J.S.**, Mitogenic signaling of insulin-like growth factor I in MCF-7 human breast cancer cells requires phosphatidylinositol 3-kinase and is independent of mitogen-activated protein kinase, *J. Biol. Chem.*, **272**: 49,31163-31171
30. **Dethlefsen S.M., Shepro D., D'Amore P.A.**, Arachidonic acid metabolites in bFGF-, PDGF-, and serum-stimulated vascular cell growth, *Exp. Cell. Res.*, **212**: 262-273, 1994
31. **Bang Y-J., Pirnia F., Fang W-G., Kang W.K., Sartor O., Whitesell L, Ha M.J., Tsokos M., Sheahan M.D., Nguyen P., Niklinski W.T., Myers C.E., Trepel J.B.**, Terminal neuroendocrine differentiation of human prostate carcinoma cells in response to increased intracellular cyclic AMP, *Proc. Natl. Acad. Sci. USA*, **91**: 5330-5334, 1994
32. **Shah G.V., Rayford W., Noble M.J., Austenfeld M., Weigel J., Vamos S., Mebust W.K.**, Calcitonin stimulates growth of human prostate cancer cells through receptor-mediated increase in cyclic adenosine 3', 5' -monophosphates and cytoplasmic Ca<sup>2+</sup> transients. *Endocrinol.*, **134**: 2, 596-602, 1994